

# RSC Advances



This is an *Accepted Manuscript*, which has been through the Royal Society of Chemistry peer review process and has been accepted for publication.

*Accepted Manuscripts* are published online shortly after acceptance, before technical editing, formatting and proof reading. Using this free service, authors can make their results available to the community, in citable form, before we publish the edited article. This *Accepted Manuscript* will be replaced by the edited, formatted and paginated article as soon as this is available.

You can find more information about *Accepted Manuscripts* in the [Information for Authors](#).

Please note that technical editing may introduce minor changes to the text and/or graphics, which may alter content. The journal's standard [Terms & Conditions](#) and the [Ethical guidelines](#) still apply. In no event shall the Royal Society of Chemistry be held responsible for any errors or omissions in this *Accepted Manuscript* or any consequences arising from the use of any information it contains.

## ARTICLE

Cite this: DOI: 10.1039/x0xx00000x

Received 00th January 2012,

Accepted 00th January 2012

DOI: 10.1039/x0xx00000x

www.rsc.org/

## Hierarchical Fe<sub>3</sub>O<sub>4</sub>@titanate microspheres with superior removal capability for water treatment: In-situ growth and structure tailoring via hydrothermal assisted etching

Liang Shi <sup>a</sup>, Bohua Dong <sup>b,\*</sup>, Rongjie Gao <sup>b</sup>, Ge Su <sup>b</sup>, Wei Liu <sup>b</sup>, Chenghui Xia <sup>a,c</sup>, Fenghuan Zhao <sup>b</sup>, Lixin Cao <sup>b,\*</sup>

Hierarchical flower-like Fe<sub>3</sub>O<sub>4</sub>@titanate microspheres with ultrathin nanosheets-assembled shell were fabricated via an effective step-by-step approach. Superparamagnetic Fe<sub>3</sub>O<sub>4</sub> microspheres pre-formed were used as templates for perfect deposition of the following coatings. Silica middle layer was introduced by Stöber method in order to direct the formation of amorphous titania coverage via the hydrolysis of tetraisopropyl titanate. Under alkaline hydrothermal environment, titanate nanosheets crystallized and grew in situ attaching on the surface of Fe<sub>3</sub>O<sub>4</sub> spheres, generating the flower-like microspheres which exhibit excellent adsorption properties. Meanwhile, the hierarchical structures can be tailored by varying the hydrothermal temperature and alkalinity, and the roles of sodium hydroxide and hydrogen peroxide were proposed.

### Introduction

One-dimensional titanate nanostructures constructed via a modified Kasuga's method <sup>1</sup> have attracted much attention in recent years for their potential applications, such as catalysis <sup>2</sup>, hydrogen storage <sup>3</sup>, as sensors <sup>4</sup> and as adsorbents <sup>5</sup>. Due to the lamellar structure with abundant confined sodium ions, titanate nanostructures are also prevalent in Li-ion batteries <sup>6</sup>. Meanwhile, the non-toxicity makes titanate ideal for use as carriers in bio-applications, for example, protein separation <sup>7</sup>. Unfortunately, the tendency of these one-dimensional structures to form bundles or random aggregates via an uncontrollable hydrothermal process was inevitable, limiting the optimal performance. As a consequence, researchers are focusing their attention on fabricating hierarchical structures assembled from one-dimensional titanate blocks, generating better capabilities, especially in the field of Li-batteries <sup>8</sup> and DSSCs <sup>9</sup>. Many attempts have been made to fabricate the hierarchical structures, where SiO<sub>2</sub> or some colloidal particles are often used as templates <sup>10</sup>. Multifunctional hierarchical structures would be

simultaneously obtained if the templates were replaced by specific functional particles. Magnetic materials, Fe<sub>3</sub>O<sub>4</sub> for example, have attracted much attention due to their selective separation, controllable drug delivery and nanocatalyst recycling <sup>11</sup>. Coincidentally, not only does hierarchical titanate match these potential applications quite well, but also Fe<sub>3</sub>O<sub>4</sub> microspheres synthesized via the solvothermal approach <sup>12-14</sup> are natural templates for their regular shape. Many studies have been conducted to achieve multifunctional materials using spherical Fe<sub>3</sub>O<sub>4</sub> as templates, but they still remain at the stage of core-shell structures with simple treatment. Therefore, controllable synthesis and structure tailoring based on magnetic titanates to form hierarchical structures still remain formidable challenges.

Several hierarchical titanate or titania structures combined with magnetic components have been prepared using various strategies. Xuan et al <sup>15</sup> obtained magnetic Fe<sub>3</sub>O<sub>4</sub>/TiO<sub>2</sub> hollow spheres by using PSA as templates, and the spheres exhibited good photocatalytic activity towards RhB, while the template-induced synthesis seemed complicated and the magnetization was quite weak due to small

Fe<sub>3</sub>O<sub>4</sub> particles. Zhao and co-workers<sup>16</sup> reported a facile route to synthesize magnetic yolk-shell titanate microspheres, but the preparation was time-consuming and required extreme concentrated basic conditions. Likewise, the work reported by Che et al<sup>17</sup> proposed the microwave-adsorption application of hierarchical Fe<sub>3</sub>O<sub>4</sub>@TiO<sub>2</sub> yolk-shell microspheres, but the process was also conducted at high temperature and long period.

In this work, we develop a facile strategy to synthesize hierarchical nanostructure based on in-situ growth and hydrothermal assisted etching. Firstly, superparamagnetic Fe<sub>3</sub>O<sub>4</sub> microspheres were prepared via the solvothermal method. In order to obtain a firm and dense coverage of amorphous titania, silica was pre-coated and then spherical-like and small steric tetraisopropyl titanate was employed. Finally, hierarchical Fe<sub>3</sub>O<sub>4</sub>@titanate microspheres were fabricated by a hydrothermal process in an extremely short reaction period and low alkaline concentration, using hydrogen peroxide as etching agent. The key experiment variables including sodium hydroxide and hydrogen peroxide for morphology controlling have been systematically investigated. The as-synthesized hierarchical Fe<sub>3</sub>O<sub>4</sub>@titanate microspheres with uniform size, tailored shell structure, high surface area and large magnetization exhibited excellent water treatment performance with high removal capacities towards organic dyes. The Fe<sub>3</sub>O<sub>4</sub>@titanate microspheres could remove almost 85% of the methylene blue within 1 min at room temperature, and adsorption equilibrium reached within 10 min. Furthermore, successful access to these rational designed hierarchical microspheres will make it possible for their potential applications in energy storage, catalysis, and sensing.

## Experimental

### Chemicals

Poly (4-styrenesulfonic acid-co-maleic acid) sodium salt (PSSMA, SS:MA=1:1, Mw~20,000), titanium isopropoxide (TTIP, 95%), and sodium acetate anhydrous were purchased from Aladdin Chemical Reagent Co. Iron(III) chloride hexahydrate, potassium chloride, sodium hydroxide, ethylene glycol, tetraethyl orthosilicate (TEOS), ethanol, ammonium hydroxide (25~28wt%) and hydrogen peroxide aqueous solution (≥30%) were all analytical grade and purchased from Sinopharm Chemical Reagent Co., Ltd. The ultra-purity water used in the experiment was produced by Water Purification System (GWA-UN1-F20, Beijing Purkinje General Instrument Co., Ltd.).

### Synthesis of superparamagnetic Fe<sub>3</sub>O<sub>4</sub> microspheres

The highly water-soluble and negatively charged superparamagnetic Fe<sub>3</sub>O<sub>4</sub> microspheres were synthesized via hydrothermal method reported by Gao et al<sup>18</sup>. Briefly, 0.5 g of PSSMA was dissolved in ethylene glycol (20 mL) under magnetic stirring to form a transparent solution, followed by the addition of FeCl<sub>3</sub>·6H<sub>2</sub>O(0.54 g). When a homogeneous red brown solution was obtained, sodium acetate (1.5 g) was then added. The obtained colloidal precursors were transferred and sealed into a Teflon-lined stainless-steel autoclave (50 mL) and heated at 200°C for 10 h. After reaction and cooling down to ambient temperature, the black products were isolated by a magnet and washed for five times with deionized water, and then dried in vacuum for 12 h.

### Synthesis of Fe<sub>3</sub>O<sub>4</sub>@SiO<sub>2</sub> microspheres

The core-shell Fe<sub>3</sub>O<sub>4</sub>@SiO<sub>2</sub> microspheres were prepared via traditional Stöber method<sup>19</sup> as follows. The as-prepared Fe<sub>3</sub>O<sub>4</sub> microspheres (150 mg) were dispersed in absolute ethanol (95 mL) contained in a three-neck round-bottom flask under ultrasound for 15min. Afterward, 21.6 mL of deionized water and 585 μL of concentrated ammonia were dropped into the solution under mechanical stirring. Finally, 3.33mL of TEOS was pre-dissolved in 5 mL of ethanol, and mixture was slowly added into the flask in three equal lots. After the reaction was proceeded for 18 h under continuous stirring, the resultant Fe<sub>3</sub>O<sub>4</sub>@SiO<sub>2</sub> microspheres were washed by ethanol and deionized water for 3 times, respectively. The Fe<sub>3</sub>O<sub>4</sub>@SiO<sub>2</sub> microspheres were redispersed in 30 mL of ethanol for further use.

### Amorphous titania coating

The Fe<sub>3</sub>O<sub>4</sub>@SiO<sub>2</sub> microspheres coated with amorphous titania were fabricated based on the controlled hydrolysis and condensation of TTIP<sup>20</sup>. One tens of the above dispersion were mixed with 92 mL of ethanol in a round-bottom flask, and the whole dispersion was ultrasonically treated for 15 min. Afterward, the flask was embedded in ice-bath and the dispersion was stirred mechanically. The addition of 80 μL of KCl (0.1 M) aqueous solution was executed when the dispersion reached steady temperature. After the water component was fully mixed in the dispersion, 320 μL of TTIP dissolved in 5 mL of ethanol were slowly added during 60 min. Then, the reaction was last for another 5 h. The resultants were washed with ethanol for 3 times and denoted as Fe<sub>3</sub>O<sub>4</sub>@SiO<sub>2</sub>@AT.

### Fabrication of Fe<sub>3</sub>O<sub>4</sub>@titanate hierarchical microspheres

The  $\text{Fe}_3\text{O}_4$ @titanate microspheres were synthesized via an alkaline hydrothermal method<sup>21</sup>. The above obtained  $\text{Fe}_3\text{O}_4$ @ $\text{SiO}_2$ @AT microspheres were fully mixed with an aqueous NaOH solution (0.1 M, 20 mL), then 300  $\mu\text{L}$  of aqueous  $\text{H}_2\text{O}_2$  solution (3wt %) was added into the mixture. Afterward, the mixture was transferred and sealed into a Teflon-lined stainless-steel autoclave (25 mL) and heated at 140 °C for 60 min. After the reaction, the autoclave was quickly cooled down and the products were washed with deionized water for 5 times.

### Characterization

X-ray diffraction (XRD) experiments were performed with a BRUKER D8 ADVANCE X-ray diffractometer fitted with  $\text{CuK}\alpha$  radiation over the  $2\theta$  ranges from 5 ° to 80 °, and the scanning speed was 4 °/min. TEM images and selected area electron diffraction (SAED) patterns of the samples were obtained on a transmission electron microscope (JEM-1200EX, JEOL) operating at 100 kV. Scanning electron microscope (SEM) inspection and element analysis were conducted using a JSM-6700F (JEOL) equipped with an Oxford INCA energy dispersive X-ray (EDX) analyzer. Fourier transform infrared (FTIR) spectra were collected with Nicolet 6700 spectrometer in the wavelength range of 4000–400  $\text{cm}^{-1}$  at 4  $\text{cm}^{-1}$

resolution. Zeta potential measurements were obtained at ambient temperature using a Zetasizer Nano ZS (Malvern) instrument. Magnetization measurements were performed on a MPMS-XL-7 (Quantum Design) superconducting quantum interference device (SQUID) magnetometer at 300 K.

### Application as adsorbents

Methylene blue solutions with various initial concentration (10, 20, 30, 40, 60, 80 and 100 mg/L) were used as probe to evaluate the adsorption properties of hierarchical  $\text{Fe}_3\text{O}_4$ @titanate. Samples (5 mg) were added into a vial with volume of 10 mL methylene blue solution for the experiment. Every 200  $\mu\text{L}$  of aliquots were taken out and diluted to 2 mL for concentration analysis at each sampling point, and the whole experimental process was conducted in a dark chamber. Sodium hydroxide solution (10 mL, 0.1 M) was used to regenerate the adsorbents, and then the  $\text{Fe}_3\text{O}_4$ @titanate was washed with water until pH of the filtrate reached neutral. The adsorption properties of as-prepared  $\text{Fe}_3\text{O}_4$  microspheres were also tested.

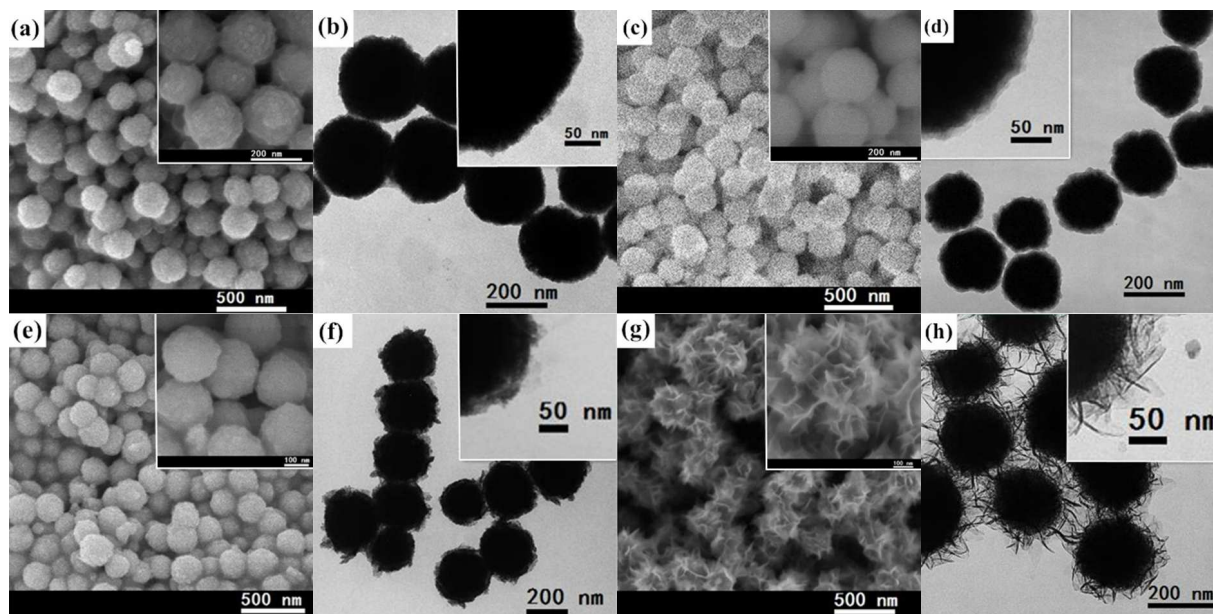


**Fig.1** SEM and TEM images of the products at each step: (a, b)  $\text{Fe}_3\text{O}_4$  microspheres (c, d)  $\text{Fe}_3\text{O}_4$ @ $\text{SiO}_2$  (e, f)  $\text{Fe}_3\text{O}_4$ @ $\text{SiO}_2$ @AT (g, h)  $\text{Fe}_3\text{O}_4$ @titanate

## Results and discussion

The magnetite particles were synthesized via a solvothermal method reported previously. The obtained  $\text{Fe}_3\text{O}_4$  particles own uniformly spherical morphology and an average diameter of  $\sim 198\text{nm}$ , as shown in Fig.1(a, b). The  $\text{Fe}_3\text{O}_4$  spheres exhibit excellent dispersibility in water, because the surface of  $\text{Fe}_3\text{O}_4$  spheres was linked with highly negatively-charged macromolecular PSSMA as the reference indicated. The zeta potential of as-prepared  $\text{Fe}_3\text{O}_4$  spheres was  $-52.0\text{mV}$  (Fig. S1), which also demonstrated a good dispersibility, favouring the subsequent coating procedures. By using the Stöber method, a smooth silica layer about  $10\text{nm}$  can be easily coated on the surface of as-prepared  $\text{Fe}_3\text{O}_4$  spheres, as shown in Fig.1(c, d). On the contrary, the  $\text{Fe}_3\text{O}_4$  surface was rough because the sub-microspheres were formed by the aggregation of many small nanocrystals with sizes of  $5\text{-}8\text{nm}$ . Moreover, the silica coatings are full of Si-OH groups, which are benefit to amorphous titania deposition<sup>22</sup>. Afterwards, the  $\text{Fe}_3\text{O}_4@\text{SiO}_2$  microspheres were coated with a layer of amorphous  $\text{TiO}_2$  through the traditional sol-gel process. Herein, tetraisopropyl titanate was used as precursor in the hydrolysis for its appropriate hydrolysis rate in neutral water without acidic or basic catalysts, which are both harmful to the existed  $\text{Fe}_3\text{O}_4$  or  $\text{SiO}_2$  components. In addition, the spherical-like and smaller steric tetraisopropyl groups are likely to produce more compacted and uniform titania layer. It can be clearly seen in Fig.1(e, f) that titania layer was successfully deposited on the surface of  $\text{Fe}_3\text{O}_4@\text{SiO}_2$  microspheres, indicating a mean thickness about  $20\text{nm}$  and a rough outer surface once again. The EDX results (Fig.S2) confirmed the content of Fe, Si and Ti were 34.13, 10.39 and 5.79 by weight, also suggesting the formation of  $\text{Fe}_3\text{O}_4@\text{SiO}_2@\text{AT}$  core-double shell microstructure. After the  $\text{Fe}_3\text{O}_4@\text{SiO}_2@\text{AT}$  microspheres were hydrothermally treated, flower-like microspheres with excellent dispersibility (Fig.S3 Zeta potential:  $-34.8\text{mV}$ ) were obtained, as shown in Fig.1(g). A bumpy shell composed by numerous nanosheets can be clearly identified, while the silica interlayer was hard to be observed by SEM or TEM. However, the EDX results (Fig.S4) confirmed there was 5.99% Si element by weight, indicating the silica interlayer was not completely removed in the hydrothermal process. Furthermore, these nanosheets possess curled edges and extend to as far as about  $50\text{nm}$ , indicating the

entire size of the flower-like microspheres about  $300\text{nm}$ , as revealed in Fig.1(h).

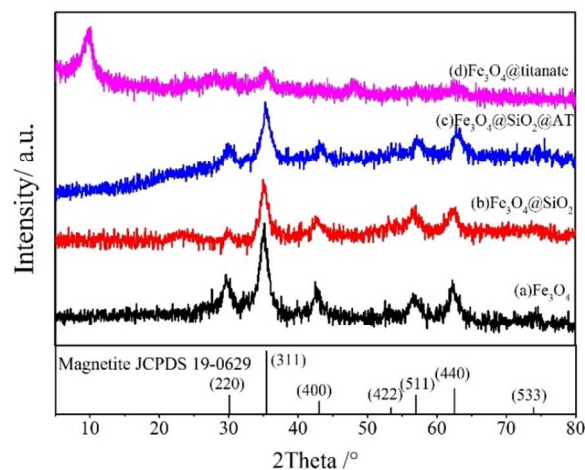


**Fig.2** XRD patterns of the products at each step: (a)  $\text{Fe}_3\text{O}_4$  microspheres (b)  $\text{Fe}_3\text{O}_4@\text{SiO}_2$  (c)  $\text{Fe}_3\text{O}_4@\text{SiO}_2@\text{AT}$  (d)  $\text{Fe}_3\text{O}_4@\text{titanate}$

XRD was used to investigate the phase composition of the samples at different stages in the entire process. Fig.2(a) shows the XRD patterns of as-prepared  $\text{Fe}_3\text{O}_4$  microspheres, and the diffraction peaks at  $2\theta=30.09^\circ$ ,  $35.42^\circ$ ,  $43.05^\circ$ ,  $53.39^\circ$ ,  $56.94^\circ$ ,  $62.52^\circ$  and  $73.95^\circ$  can be indexed as (220), (311), (400), (422), (511), (440) and (533) planes of magnetite(JCPDS 19-0629). The XRD patterns of  $\text{Fe}_3\text{O}_4@\text{SiO}_2$  and  $\text{Fe}_3\text{O}_4@\text{SiO}_2@\text{AT}$  present similar characteristics as their parent  $\text{Fe}_3\text{O}_4$ , except for a broad peak at  $2\theta=25^\circ$ , which is assigned to amorphous silica, as shown in Fig.2(b, c). However, the situation was quite different for  $\text{Fe}_3\text{O}_4@\text{titanate}$  microspheres when hydrothermal process was conducted. As Fig.2(d) indicated, a strong peak at  $9.7^\circ$  and small one at  $48.0^\circ$  can be attributed to lepidocrocite-type titanate<sup>23</sup>, while the feature of magnetite was also reserved.

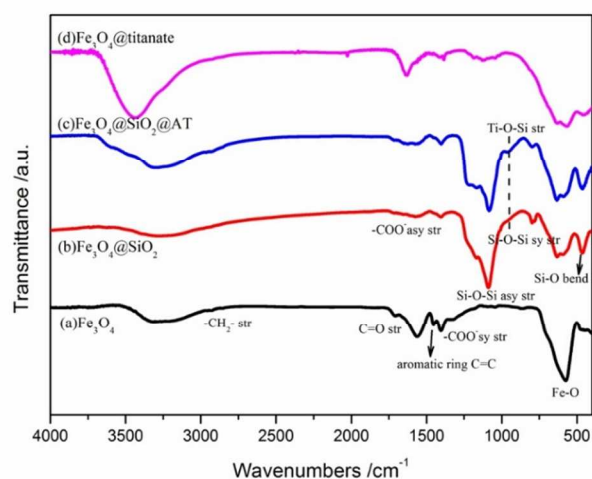


**Fig.3** FTIR spectra of the products at each step: (a)  $\text{Fe}_3\text{O}_4$  microspheres (b)  $\text{Fe}_3\text{O}_4@SiO_2$  (c)  $\text{Fe}_3\text{O}_4@SiO_2@AT$  (d)  $\text{Fe}_3\text{O}_4@titanate$

As the synthesis procedure involved the formation of several amorphous structures, FTIR analysis was performed to characterize the sequential coating and growth process. Fig.3 displays the FTIR spectra of corresponding products in the range of 400-4000  $\text{cm}^{-1}$ . As shown in Fig.3(a), the strong band at 574  $\text{cm}^{-1}$  is due to characteristic absorption peaks from the Fe-O in  $\text{Fe}_3\text{O}_4$ , while bands at 1403 and 1564  $\text{cm}^{-1}$  are assigned to symmetric and asymmetric stretching vibration of carboxylate groups, respectively, indicating the  $\text{Fe}_3\text{O}_4$  nanoparticles are bonded with PSSMA. Moreover, the stretching mode of  $-\text{CH}_2-$  (2930  $\text{cm}^{-1}$ ),  $\text{C}=\text{O}$  (1700  $\text{cm}^{-1}$ ) and aromatic ring  $\text{C}=\text{C}$  (1453  $\text{cm}^{-1}$ ) can be observed, also suggesting the existence of PSSMA reserved in the microspheres. As silica layer was coated on the surface of  $\text{Fe}_3\text{O}_4$  microspheres, the high-intensity Si-O-Si asymmetric stretching band (1093  $\text{cm}^{-1}$ ) was observed while the Fe-O bands (574  $\text{cm}^{-1}$ ) weakened, as revealed in Fig.3(b). Besides, the additional bands at 475, and 799  $\text{cm}^{-1}$ , which are associated with Si-O-Si or O-Si-O bending mode and Si-O-Si symmetric stretching vibration, respectively, can be also detected. After the hydrolysis of tetraisopropyl titanate was completed, the FTIR spectra was quite similar to that of  $\text{Fe}_3\text{O}_4@SiO_2$ , as shown in Fig.3(c). However, a new band at 947  $\text{cm}^{-1}$  can be found which is attributed to stretching vibration of Ti-O-Si, demonstrating amorphous titania indeed covered the surface of  $\text{SiO}_2$ . Fig.3(d) displays the spectra of hierarchical microspheres, and characteristics of  $\text{SiO}_2$  weaken in the hydrothermal process due to silica is susceptible to basic conditions, but still exist as mentioned above. Meanwhile, the

broad band centred at 3400  $\text{cm}^{-1}$  was assigned to O-H stretching vibration of physically absorbed water.

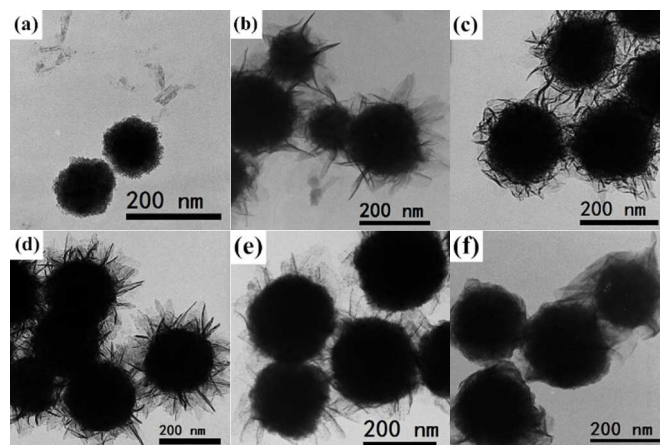


**Fig.4** TEM images of final products synthesized by different hydrothermal temperature for 60 min (a) 100 °C (b) 120 °C (c) 140 °C (d) 160 °C (e) 180 °C (f) 200 °C. In these cases,  $c(\text{NaOH})=0.1$  M.

In order to investigate the effects of hydrothermal temperature on the etching process and structure of the final products, we conducted a series of experiments with temperature range of 100-200 °C. Fig.4(a) shows bare  $\text{Fe}_3\text{O}_4$  microspheres and dislocated Ti-fragments were obtained when hydrothermal process was conducted at a quite low temperature (100 °C). A plausible explanation was that the crystallization of amorphous titania was extremely slow while silica coating was dissolved in alkaline condition<sup>24</sup>, and titania skin was peeled off into environment in the form of partially crystallized fragments. It can be seen from Fig.4(b, c) that flower-like  $\text{Fe}_3\text{O}_4@titanate$  microspheres were formed when hydrothermal temperature was increased to 120°C and 140°C, but there were still some dislocated components at 120°C because of slower reaction. However, some nanoparticles were observed attaching to titanate nanosheets as temperature was further increased to 160, as illustrated in Fig.4(d). At the same time, we can also identify the nanoparticles from TEM images in Fig.4(e) when temperature was 180°C. The phenomenon can be interpreted as  $\text{Fe}_3\text{O}_4$  primary particle self-assembled in the microspheres fell off under harshly etching at higher temperature. Moreover, titanate nanosheets became fewer and straighter due to a faster reaction rate. When the hydrothermal temperature was set as high as 200°C, no flower-like products were obtained, as

revealed in Fig.4(f). The amorphous titania coating crystallized and grew at such a high rate that adjacent nanosheets interacted with each other, yielding a disordered shell.

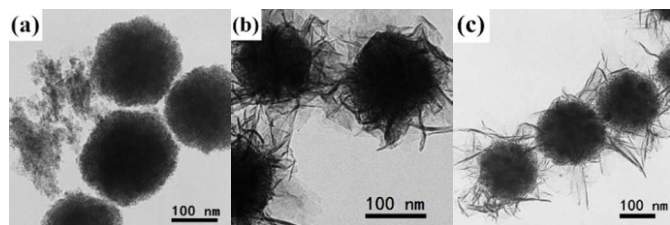


**Fig.5** TEM images of obtained products synthesized at 140 °C for 60 min with various concentration of sodium hydroxide (a) 0 M (b) 0.1 M (c) 0.5 M

To understand the role of sodium hydroxide in the formation of titanate nanosheets, a control experiment was also conducted by varying the concentration of sodium hydroxide aqueous solution. As shown in Fig.5(a-c), various morphologies of final products were obtained by adjusting  $c(\text{NaOH})$  to 0 M, 0.1 M and 0.5 M, respectively. As demonstrated by previous research<sup>21</sup>, hydrogen peroxide only facilitates curling the titanate nanosheets, and has no effects on the formation of the nanosheets. Herein, hydroxide peroxide was added in all the experiments and the concentration was fixed. When no sodium hydroxide was introduced, bare  $\text{Fe}_3\text{O}_4$  microspheres together with some aggregates of nanoparticles were observed, no sheet-like structures were found, as shown in Fig.5(a). Interestingly, the role of sodium hydroxide and hydrogen peroxide can be realized by this single experiment. As no sodium hydroxide was in the reaction and the silica-titania double-shell was peeled off yet, hydrogen peroxide can be identified as etching agent. Meanwhile, no attached or dislocated sheet-like products were obtained, proving sodium hydroxide plays significant role in formation of titanate nanosheets, as testified by XRD measurements. Moreover, the role of sodium hydroxide can be further certified because longer nanosheets formed at higher concentration, as Fig.5(c) revealed. Under a relative sufficient concentration of reactant, the Ostwald ripening process was likely to be triggered to form much large and sparse nanosheets, instead of relatively small and dense ones.

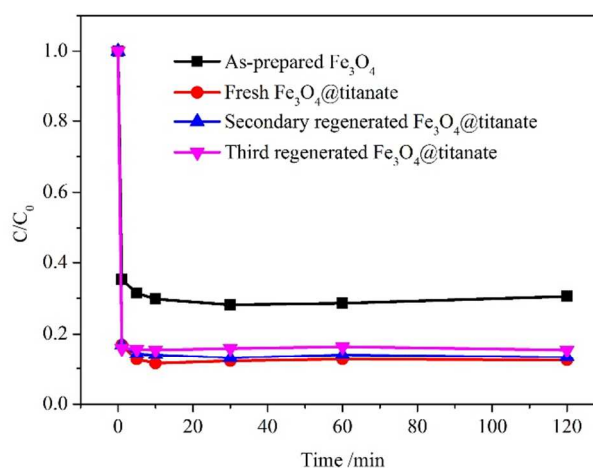


**Fig.6** Adsorption properties of  $\text{Fe}_3\text{O}_4$ , new as-obtained  $\text{Fe}_3\text{O}_4$ @titanate microspheres and regenerated materials, respectively. (Experimental conditions: Methyl blue  $C_0=30\text{mg/L}$ , adsorbents dosage= $0.5\text{g/L}$ )

Recently, many investigations show that contaminants in freshwater could be partially removed by nano-adsorbents or nanocatalysts<sup>25, 26</sup>.  $\text{Fe}_3\text{O}_4$  microspheres were previously demonstrated as good adsorbents for azo-dyes, and can be recovered efficiently through facile magnetic separation<sup>27</sup>. Inspired by the hierarchical structure and magnetic properties, we expect the  $\text{Fe}_3\text{O}_4$ @titanate microspheres possess better performance as recyclable adsorbents. Fig.6 shows the adsorption plots of methylene blue by as-prepared  $\text{Fe}_3\text{O}_4$ ,  $\text{Fe}_3\text{O}_4$ @titanate microspheres (140°C, 0.1M NaOH) and regenerated materials, respectively. Surprisingly, the  $\text{Fe}_3\text{O}_4$ @titanate microspheres could remove almost 85% of the methylene blue within 1 min at room temperature, and adsorption equilibrium reached within 10 min. Moreover, the regenerated hierarchical  $\text{Fe}_3\text{O}_4$ @titanate microspheres could also absorb more than 80% of the methylene blue, while the new as-prepared  $\text{Fe}_3\text{O}_4$  reached 70% only. Methylene blue is cationic dye and the electrostatic attractions play significant role in adsorption process. As the as-prepared  $\text{Fe}_3\text{O}_4$  microspheres benefit from more negative surface ( $-52.0\text{mV}$  vs.  $-34.8\text{mV}$  for  $\text{Fe}_3\text{O}_4$ @titanate), then the excellent  $\text{Fe}_3\text{O}_4$ @titanate microspheres adsorbents were attributed to the hierarchical structures.

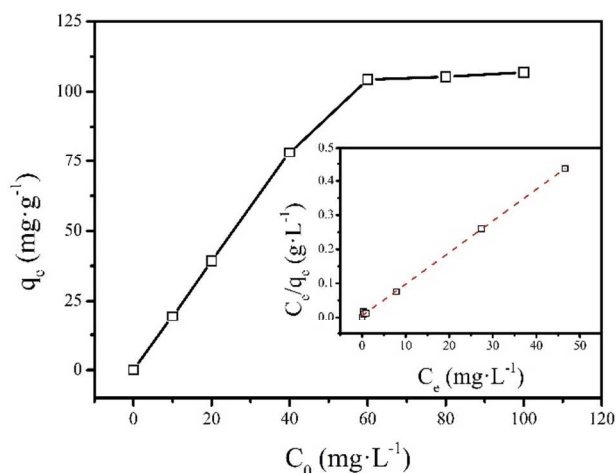


**Fig.7** Adsorption isotherm of MB by fresh-prepared  $\text{Fe}_3\text{O}_4$ @titanate microspheres. Inset: Linearized Langmuir isotherm for MB adsorption.

In order to investigate the adsorption capacity of the hierarchical  $\text{Fe}_3\text{O}_4$ @titanate microspheres, the equilibrium adsorption experiments were conducted by varying initial MB concentrations. As shown in Fig.7, the adsorption capacity for MB was monotonously increased when the initial concentration was lower than 60mg/L. However, the equilibrium adsorption capacity tended to be saturated as the initial MB concentration was further increased. Two equations, Langmuir and Freundlich isotherms models, were employed to analyze the adsorption data. As inset of Fig.7 shows, the adsorption behaviour of  $\text{Fe}_3\text{O}_4$ @titanate could be described by Langmuir model, while the experimental data deviated from the Freundlich equation, indicating a monolayer adsorption process of MB by  $\text{Fe}_3\text{O}_4$ @titanate. As methylene blue is a cationic dye, there exist electrostatic attraction between MB and negatively charged  $\text{Fe}_3\text{O}_4$ @titanate microspheres, and the adsorbed MB molecules have a repulsive force on the others. Moreover, the maximum adsorption capacity can be calculated by the slope of the linearized Langmuir isotherm ( $R^2=0.99918$ ), which was up to 108.11mg/g.

**Table.1** Adsorption capacity of different magnetic adsorbents for MB.

Adsorbents	Initial MB Concentration(mg/L)	$q_m$ (mg/g)	Ref.
$\text{Fe}_3\text{O}_4$ @C Nanospheres	40-80	45.2	28
PAA/MnFe <sub>2</sub> O <sub>4</sub>	8.3	53.3	29
$\text{Fe}_3\text{O}_4$ -GO-CNTs	10-35	65.8	30
$\text{Fe}_3\text{O}_4$ -GO	10-400	526.3	31

Table.1 lists a comparison of maximum adsorption capacities of magnetic adsorbents for MB removal previously reported. It can be seen that  $\text{Fe}_3\text{O}_4$ @titanate microspheres have higher adsorption ability than most of those in other literatures. Although the adsorption capacity was smaller than that of previous work by Cui<sup>31</sup>, which showed a capacity of 526.3mg/g of MB by  $\text{Fe}_3\text{O}_4$ -graphene oxide composites, the robust titanate seems to be easier to recycle and can be expanded to apply in catalysis as owning that potential mentioned above.

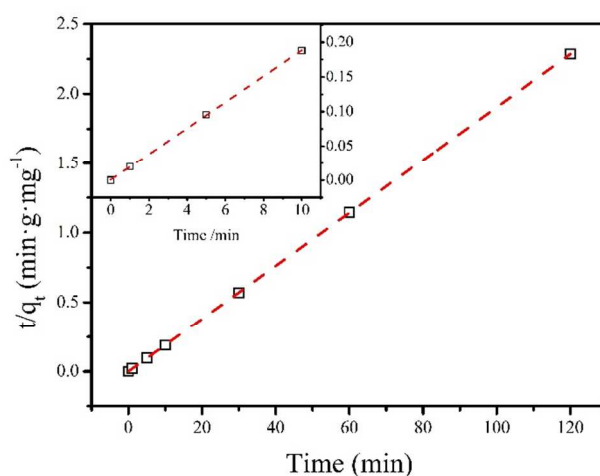


**Fig.8** Linearized pseudo-second-order kinetics model of MB by fresh-prepared  $\text{Fe}_3\text{O}_4$ @titanate microspheres (initial MB concentration: 30mg/L).

According to previous report<sup>32</sup>, the adsorption kinetics process of methylene blue by titanate conformed to the pseudo-second-order model. Fig.8 shows the linearized plots of the adsorption process, and plots by partial data were also displayed in the inset as the actual adsorption equilibrium reached within 10min. As both of the plots exhibited excellent linearity, the adsorption kinetics behaviour of the hierarchical  $\text{Fe}_3\text{O}_4$ @titanate microspheres fitted the pseudo-second-order model, and the apparent rate ( $k_2=4.541$ ) can be calculated from the intercept.

## Conclusions

We have demonstrated an in-situ growth and hydrothermal assisted etching strategy to fabricate flower-like  $\text{Fe}_3\text{O}_4$ @titanate microspheres with nanosheets-assembled shell. The obtained hierarchical structure reserves the superparamagnetic characteristics, possesses promising application as adsorbents and can be tailored by varying temperature or alkalinity. The preparation procedure is free of organic directing agents and high alkalinity, while accompanied by a time-saving hydrothermal process. This ideal synthetic strategy is expected valid to direct to design other hierarchical composites.

## Acknowledgements

This research was supported by the National Natural Science Foundation of China (No. 51172218, 51372234, 21301187).

## Notes and references

<sup>a</sup> College of Chemistry and Chemical Engineering, Ocean University of China, Qingdao 266100, PR China

<sup>b</sup> Institute of Materials Science and Engineering, Ocean University of China, Qingdao 266100, PR China

<sup>c</sup> Debye Institute, Utrecht University, Princetonplein 1, 3584 CC Utrecht, Netherlands

† Electronic Supplementary Information (ESI) available: Zeta potential of  $\text{Fe}_3\text{O}_4$  and  $\text{Fe}_3\text{O}_4$ @titanate microspheres, EDX results of  $\text{Fe}_3\text{O}_4$ @ $\text{SiO}_2$ @AT and  $\text{Fe}_3\text{O}_4$ @titanate, and magnetic properties of  $\text{Fe}_3\text{O}_4$ @titanate microspheres. See DOI: 10.1039/b000000x/

- 1 T. Kasuga, M. Hiramatsu, A. Hoson, T. Sekino and K. Niihara, *Langmuir*, 1998, **14**, 3160-3163.
- 2 M. Kitano, K. Nakajima, J. N. Kondo, S. Hayashi and M. Hara, *J Am Chem Soc*, 2010, **132**, 6622-6623.
- 3 D. V. Bavykin, A. A. Lapkin, P. K. Plucinski, J. M. Friedrich and F. C. Walsh, *J Phys Chem B*, 2005, **109**, 19422-19427.
- 4 E. Horváth, P. R. Ribič, F. Hashemi, L. Forró and A. Magrez, *J Mater Chem*, 2012, **22**, 8778-8784.
- 5 S. N. Britvin, A. Lotnyk, L. Kienle, S. V. Krivovichev and W. Depmeier, *J Am Chem Soc*, 2011, **133**, 9516-9525.
- 6 Y. Tang, Y. Zhang, J. Deng, D. Qi, W. R. Leow, J. Wei, S. Yin, Z. Dong, R. Yazami, Z. Chen and X. Chen, *Angew Chem Int Ed*, 2014, **53**, 13488-13492.
- 7 W. J. Dong, Y. J. Zhu, H. D. Huang, L. S. Jiang, H. J. Zhu, C. R. Li, B. Y. Chen, Z. Shi and G. Wang, *J Mater Chem A*, 2013, **1**, 10030-10036.
- 8 J. Cheng, R. C. Che, C. Y. Liang, J. W. Liu, M. Wang and J. J. Xu, *Nano Res*, 2014, **7**, 1043-1053.
- 9 Z. H. Liu, X. J. Su, G. L. Hou, S. Bi, Z. Xiao and H. P. Jia, *Nanoscale*, 2013, **5**, 8177-8183.
- 10 J. Wang, T. Qiu, X. Chen, Y. L. Lu and W. S. Yang, *J Power Sources*, 2014, **268**, 341-348.
- 11 S. Laurent, D. Forge, M. Port, A. Roch, C. Robic, L. V. Elst and R. N. Muller, *Chem. Rev.*, 2008, **108**, 2064-2110.
- 12 S. H. Xuan, Y. J. Wang, J. C. Yu and K. C. Leung, *Chem Mater*, 2009, **21**, 5079-5087.
- 13 W. Cheng, K. B. Tang, Y. X. Qi, J. Sheng and Z. P. Liu, *J Mater Chem*, 2010, **20**, 1799-1805.
- 14 J. P. Ge, Y. X. Hu, M. Biasini, W. P. Beyermann and Y. D. Yin, *Angew Chem Int Ed*, 2007, **46**, 4342-4345.
- 15 S. H. Xuan, W. Q. Jiang, X. L. Gong, Y. Hu and Z. Y. Chen, *J Phys Chem C*, 2009, **113**, 55-558.
- 16 W. Li, Y. H. Deng, Z. X. Wu, X. F. Qian, J. P. Yang, Y. Wang, D. Gu, F. Zhang, B. Tu and D. Y. Zhao, *J Am Chem Soc*, 2011, **133**, 15830-15833.
- 17 J. W. Liu, J. J. Xu, R. C. Che, H. J. Chen, M. M. Liu and Z. W. Liu, *Chem Eur J*, 2013, **19**, 6746-6752.
- 18 J. N. Gao, X. Z. Ran, C. M. Shi, H. M. Cheng, T. M. Cheng and Y. P. Su, *Nanoscale*, 2013, **5**, 7026-7033.
- 19 W. Stöber, A. Fink and E. Bohn, *J Colloid Interface Sci*, 1968, **26**, 62-69.
- 20 Y. W. Wang, H. Xu, X. B. Wang, X. Zhang, H. M. Jia, L. Z. Zhang and J. R. Qiu, *J Phys Chem B*, 2006, **110**, 13835-13840.

## Journal Name

- 21 Y. F. Tang, L. Yang, J. Z. Chen and Z. Qiu, *Langmuir*, 2010, **26**, 10111-10114.
- 22 X. X. Yu, S. W. Liu and J. G. Yu, *Appl Catal B: Environ*, 2011, **104**, 12-20.
- 23 R. Z. Ma, K. Fukuda, T. Sasaki, M. Osada and Y. Bando, *J Phys Chem B*, 2005, **109**, 6210-6214.
- 24 Q. Zhang, T. R. Zhang, J. P. Ge and Y. D. Yin, *Nano Lett*, 2008, **8**, 2867-2871.
- 25 W. Q. Cai, J. G. Yu and M. Jaroniec, *J Mater Chem*, 2010, **20**, 4587-4594.
- 26 J. B. Fei, Y. Cui, X. H. Yan, W. Qi, Y. Yang, K. W. Wang, Q. He and J. B. Li, *Adv Mater*, 2008, **20**, 452-456.
- 27 M. R. Gao, S. R. Zhang, J. Jiang, Y. R. Zheng, D. Q. Tao and S. H. Yu, *J Mater Chem*, 2011, **21**, 16888-16892.
- 28 Y. M. Shao, L. C. Zhou, C. Bao and J. J. Ma, *Carbon*, 2015, **89**, 378-391.
- 29 W. Wang, Z. Ding, M. H. Cai, H. T. Jian, Z. Q. Zeng and F. Li, *Appl Surf Sci*, 2015, **346**, 348-353.
- 30 P. F. Wang, M. H. Cao, C. Wang, Y. H. Ao, J. Hou and J. Qian, *Appl Surf Sci*, 2014, **290**, 116-124.
- 31 L. M. Li, X. Y. Guo, Q. Wei, Y. G. Wang, L. Gao, L. G. Yan, T. Yan and B. Du, *J Colloid Interface Sci*, 2015, **439**, 112-120.
- 32 M. Feng, W. You, Z. S. Wu, Q. D. Chen and H. B. Zhan, *ACS Appl Mater & Interfaces*, 2013, **5**, 12654-12662.

## A table of contents entry



Superparamagnetic hierarchical  $\text{Fe}_3\text{O}_4$ @titanate microspheres synthesized via a hydrothermal process exhibit rapid adsorption behavior and can be used as recyclable adsorbents.